

Measurement of the xF_3 and F_2 structure functions in the low Q^2 region with the IHEP-JINR neutrino detector

A.V. Sidorov¹, V.B. Anykeyev², Y.A. Batusov¹, S.A. Bunyatov¹, A.A. Borisov², N.I. Bozhko², S.K. Chernichenko², G.L. Chukin², O.Y. Denisov¹, R.M. Fachrutdinov², V.N. Goryachev², M.Y. Kazarinov¹, M.M. Kirsanov², O.L. Klimov¹, A.I. Kononov², A.S. Kozhin², A.V. Krasnoperov¹, V.I. Kravtsov², V.E. Kuznetsov¹, V.V. Lipajev², A.I. Mukhin², Y.A. Nefedov¹, B.A. Popov¹, S.N. Prakhov¹, Y.I. Salomatin², V.I. Snyatkov¹, Y.M. Sviridov², V.V. Tereshchenko¹, V.L. Tumakov², V.Y. Valuev¹, A.S. Vovenko²

¹ Joint Institute for Nuclear Research, 141980 Dubna Moscow Region, Russia

² Institute for High Energy Physics, 142284 Protvino Moscow Region, Russia

Received: 3 November 1998 / Revised version: 27 May 1999 / Published online: 12 August 1999

Abstract. The isoscalar structure functions xF_3 and F_2 are measured as functions of x averaged over all Q^2 permissible for the range of 6 to 28 GeV of incident neutrino (anti-neutrino) energy at the IHEP-JINR neutrino detector. The QCD analysis of the xF_3 structure function yields $\Lambda_{\overline{\text{MS}}}^{(4)} = (411 \pm 200)$ MeV under the assumption of the validity of QCD in the region of low Q^2 . The corresponding value of the strong interaction constant $\alpha_S(M_Z) = 0.123_{-0.013}^{+0.010}$ agrees with the recent result of the CCFR collaboration and with the combined LEP/SLC result.

1 Introduction

The data on deep-inelastic neutrino and anti-neutrino scattering in a wide region of momentum transfer provide a reliable basis for a precise verification of the QCD predictions [1]. In this paper we present the measurements of the xF_3 and F_2 structure functions (SF) and the QCD analysis of xF_3 in the kinematic region of relatively small momentum transfer $0.55 < Q^2 < 4.0$ GeV². The value of the strong interaction constant $\alpha_S(M_Z)$ is also evaluated and compared with the results of other experiments.

2 Data samples

The analysis is based on data collected with three independent exposures of the IHEP-JINR neutrino detector [2] to the wide-band neutrino and anti-neutrino beams [3] of the Serpukhov U-70 accelerator. The exposure to the anti-neutrino beam ($\bar{\nu}_\mu$ exposure) was performed at the proton beam energy $E_p = 70$ GeV, whereas the two ν_μ -exposures were carried out at $E_p = 70$ GeV and at $E_p = 67$ GeV. The energy of the resulting ν_μ ($\bar{\nu}_\mu$) was in the range of $6 < E_{\nu(\bar{\nu})} < 28$ GeV.

The experimental set-up and the selection criteria of charged current (CC) neutrino and anti-neutrino interactions are discussed in [4]. We restricted the range of measurements to $W^2 > 1.7$ GeV² in order to reject quasi-elastic and resonance events and select mainly deep-inelastic neutrino and anti-neutrino interactions. The number of

Send offprint requests to: sidorov@thsun1.jinr.ru

Table 1. Summary of the exposures

Beam	$\bar{\nu}_\mu$	ν_μ	ν_μ
E_p , GeV	70	70	67
$N_{\text{p.o.t.}} \times 10^{17}$	2.86	1.05	2.11
Final statistics	741	2 139	3 848
$\langle Q^2 \rangle$, GeV ²	1.2	2.3	

protons on target (p.o.t.) for each exposure, the selected number of ν_μ CC and $\bar{\nu}_\mu$ CC events and the mean values of Q^2 for the three data samples are given in Table 1.

3 Data analysis

The SF's were measured as functions of x averaged over all Q^2 permissible for the energy range $6 < E_{\nu(\bar{\nu})} < 28$ GeV. The events were binned in intervals of x , and the values of xF_3 and F_2 were calculated in these intervals.

The number of ν_μ interactions, n^ν , and $\bar{\nu}_\mu$ interactions, $n^{\bar{\nu}}$, in a given bin of x is a linear combination of the average values $\{F_2\}$ and $\{xF_3\}$ of the respective SF in this bin (we assume invariance under charge conjugation):

$$\begin{aligned} n^{\bar{\nu}} &= a^{\bar{\nu}} \cdot \{F_2\} - b^{\bar{\nu}} \cdot \{xF_3\}, \\ n_{1,2}^\nu &= a_{1,2}^\nu \cdot \{F_2\} + b_{1,2}^\nu \cdot \{xF_3\}. \end{aligned}$$

The subscripts 1 and 2 correspond to the ν_μ -exposures at $E_p = 70$ GeV and $E_p = 67$ GeV, respectively. The quanti-

Table 2. The isoscalar structure functions F_2 and $x\bar{F}_3$ obtained with the assumption of $R = 0$. The difference ΔF_2 between the values of F_2 obtained with $R = 0.1$ and with $R = 0$ is also presented. The bin edges are at $x = 0.02, 0.1, 0.2, 0.3, 0.4, 0.5$ and 0.65 . The shown systematic errors do not include the normalization error of 4% for F_2 and 11% for $x\bar{F}_3$ originating from the uncertainties in the ν_μ and $\bar{\nu}_\mu$ flux prediction [13]

$\langle x \rangle$	$\langle Q^2 \rangle$, GeV ²	F_2	stat	syst	ΔF_2	$x\bar{F}_3$	stat	syst
0.052	0.55	1.169	0.039	0.047	0.023	0.445	0.458	0.062
0.148	1.4	1.097	0.036	0.022	0.022	0.583	0.087	0.017
0.248	2.2	0.894	0.032	0.018	0.019	0.622	0.075	0.019
0.346	2.9	0.576	0.028	0.017	0.013	0.556	0.109	0.011
0.447	3.4	0.390	0.025	0.012	0.009	0.336	0.070	0.007
0.563	4.0	0.182	0.017	0.004	0.004	0.177	0.117	0.005

ties $a^{\nu(\bar{\nu})}$ and $b^{\nu(\bar{\nu})}$ are the integrals (“flux integrals”) of products of the differential neutrino (anti-neutrino) flux $\phi^{\nu(\bar{\nu})}(E)$ and the known factors depending on the scaling variables x and y , as given by the standard form of the differential cross-section for deep-inelastic $\nu_\mu(\bar{\nu}_\mu)$ scattering off an isoscalar target:

$$a^{\nu(\bar{\nu})} = N \frac{G^2 M}{\pi} \int \left(1 - y - \frac{Mxy}{2E} + \frac{y^2}{2(R+1)} \right) \times E \phi^{\nu(\bar{\nu})}(E) dx dy dE,$$

$$b^{\nu(\bar{\nu})} = N \frac{G^2 M}{\pi} \int y \left(1 - \frac{y}{2} \right) E \phi^{\nu(\bar{\nu})}(E) dx dy dE.$$

Here N is the number of nucleons in the fiducial volume of the detector and the parameter $R = (F_2 - 2xF_1)/2xF_1$ measures the violation of the Callan–Gross relation [5].

The number $n^{\nu(\bar{\nu})}$ of neutrino (anti-neutrino) interactions in a given bin of x was obtained from the measured number of neutrino (anti-neutrino) events in this bin corrected for acceptance, smearing effects arising from Fermi motion and measurement uncertainties, radiative effects (following the prescription given by De Rújula et al. [6]) and target non-isoscalarity (assuming $d_v/u_v = 0.5$) [7]. To determine appropriate correction factors, the Monte Carlo simulation of the experimental set-up has been carried out using the CATAS program [8]. We used the Buras and Gaemers (BEBC) parameterization [9] for the quark distributions. The charm quark content of the nucleon was assumed to be zero. The kinematic suppression of $d \rightarrow c$ and $s \rightarrow c$ transitions was taken into account assuming slow rescaling [10] and the charm and strange quark masses of $m_c = 1.25$ GeV and $m_s = 0.25$ GeV respectively. The Fermi motion of nucleons was simulated according to [11]. The details of the Monte Carlo simulation are described in [4, 12].

The number of interactions in a given bin of x is subjected to kinematic constraints imposed by the cuts on the muon momentum ($p_\mu > 1$ GeV/c [4]), on the neutrino (anti-neutrino) energy ($6 < E_{\nu(\bar{\nu})} < 28$ GeV) and on the invariant mass square of the hadronic system ($W^2 > 1.7$ GeV²). These constraints were taken into account in

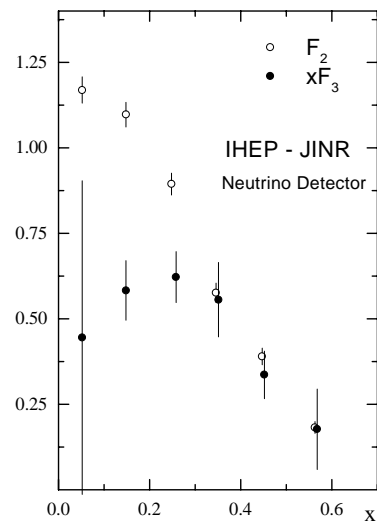


Fig. 1. The measured x -dependence of the isoscalar structure functions $F_2(x)$ and $x\bar{F}_3(x)$. The statistical and systematic errors are added in quadrature (the normalization errors of 4% for F_2 and 11% for $x\bar{F}_3$ are not shown)

the calculation of the flux integrals by an appropriate modification of the volume of integration.

The measured values of F_2 and $x\bar{F}_3$ structure functions are given in Table 2 and in Fig. 1.

The systematic errors presented in Table 2 come from the uncertainties in the knowledge of the neutrino flux and cross-sections [4], imperfect detector calibration and uncertainties in the correction factors due to the choice of the input quark distributions. The overall normalization error, originating from the uncertainties in the ν_μ and $\bar{\nu}_\mu$ flux prediction [13], was estimated to be 4% for F_2 and 11% for $x\bar{F}_3$. The correction factor uncertainties were evaluated by repeating the calculation of the SF using the Field–Feynman [14] and GRV [15] parameterizations of the quark distributions.

The obtained experimental data on the $x\bar{F}_3$ were then compared with the QCD prediction for the Q^2 evolution by the Jacobi polynomials method in the next-to-leading order (NLO) QCD approximation [16–18]. Performing the QCD analysis of the $x\bar{F}_3$ SF, we do not discuss here the

problem of the validity of application of perturbative QCD predictions for the kinematic region of low Q^2 and do not take into account nuclear effects, heavy quarks threshold effects and higher order QCD corrections.

In order to take into account the target mass corrections, the Nachtmann moments [19] of F_3 are expanded in powers of M_{nucl}^2/Q^2 . Retaining only the terms of the order of M_{nucl}^2/Q^2 , one has

$$M_3(N, Q^2) = M_3^{\text{QCD}}(N, Q^2) + \frac{N(N+1)}{N+2} \frac{M_{\text{nucl}}^2}{Q^2} M_3^{\text{QCD}}(N+2, Q^2). \quad (1)$$

Here $M_3^{\text{QCD}}(N, Q^2)$ are the Mellin moments of xF_3 :

$$M_3^{\text{QCD}}(N, Q^2) = \int_0^1 x^{N-2} xF_3(x, Q^2) dx, \quad (2)$$

$$N = 2, 3, \dots$$

The Q^2 evolution of the Mellin moments is defined by QCD [20, 21] and is presented here for the non-singlet case for simplicity:

$$M_3^{\text{QCD}}(N, Q^2) = \left[\frac{\alpha_s(Q_0^2)}{\alpha_s(Q^2)} \right]^{d_N} H_N(Q_0^2, Q^2) \times M_3^{\text{QCD}}(N, Q_0^2), \quad N = 2, 3, \dots \quad (3)$$

$$d_N = \gamma_N^{(0)\text{NS}} / 2\beta_0,$$

$$\beta_0 = 11 - \frac{2}{3}n_f.$$

Here $\alpha_s(Q^2)$ is the strong interaction constant, $\gamma_N^{(0)\text{NS}}$ are the non-singlet leading order anomalous dimensions and n_f is the number of flavors. The factor $H_N(Q_0^2, Q^2)$ contains all next-to-leading order QCD corrections [18, 21, 22].

The unknown coefficients $M_3^{\text{QCD}}(N, Q_0^2)$ in (3) could be parameterized as the Mellin moments of some function:

$$M_3^{\text{QCD}}(N, Q_0^2) = \int_0^1 x^{N-2} A x^b (1-x)^c dx, \quad (4)$$

$$N = 2, 3, \dots,$$

where the constants A , b and c should be determined from the fit to the data. Having defined the moments (1)–(4) and following the method discussed in [16, 17], we can write the xF_3 SF in the form

$$xF_3^{\text{QCD}}(x, Q^2) = x^\alpha (1-x)^\beta \sum_{n=0}^{N_{\text{max}}} \Theta_n^{\alpha, \beta}(x) \times \sum_{j=0}^n c_j^n(\alpha, \beta) M_3(j+2, Q^2),$$

where $\Theta_n^{\alpha, \beta}(x)$ are the Jacobi polynomials and $c_j^n(\alpha, \beta)$ are the coefficients of the expansion of $\Theta_n^{\alpha, \beta}(x)$ in powers of x :

Table 3. The results of the NLO QCD fit to the xF_3 SF data for $n_f = 4$, $Q_0^2 = 3 \text{ GeV}^2$, $N_{\text{max}} = 9$, $\alpha = 0.7$, $\beta = 3.0$

χ^2	0.22
A	10.4 (fixed)
b	0.86 ± 0.14
c	3.83 ± 0.61
$\Lambda_{\overline{\text{MS}}}^{(4)}$	$(411 \pm 200) \text{ MeV}$
$\alpha_s(M_Z)$	$0.123_{-0.013}^{+0.010}$

$$\Theta_n^{\alpha, \beta}(x) = \sum_{j=0}^n c_j^n(\alpha, \beta) x^j.$$

The accuracy of the SF approximation, better than 1%, is achieved for $N_{\text{max}} = 9$ in a wide region of the parameters α and β [17].

The higher-twist (HT) contribution is also taken into account:

$$xF_3(x, Q^2) = xF_3^{\text{QCD}}(x, Q^2) + \frac{h(x)}{Q^2},$$

where $h(x) = 0.166 - 3.746 \cdot x + 9.922 \cdot x^2 - 6.730 \cdot x^3$ is chosen by an interpolation of the NLO result for the HT contribution from [23]. This shape of $h(x)$ is in a good agreement with the theoretical prediction of [24] and with the result of [25, 26] obtained for a kinematic region with a higher Q^2 .

Using nine Mellin moments and taking into account target mass corrections, we have determined four parameters: A , b , c and the QCD parameter $\Lambda_{\overline{\text{MS}}}$ (Table 3). In order to decrease the number of free parameters we have fixed the value of the parameter A using the Gross–Llewellyn Smith sum rule Q^2 dependence: $S_{\text{GLS}} = 3(1 - \alpha_s(Q_0^2)/\pi)$ [27]. The fit was performed using the MINUIT program [28]. Three sources of errors – statistical, systematic and normalization – were added in quadrature. The errors for the free parameters corresponding to the 70% confidence level were obtained using the procedure described in [29]. A relatively good accuracy of the measurements of $\Lambda_{\overline{\text{MS}}}$ was achieved due to the high sensitivity of the QCD evolution equations to the variations of $\Lambda_{\overline{\text{MS}}}$ in the low Q^2 region ($0.55 < Q^2 < 4.0 \text{ GeV}^2$ in our case).

The value of $\alpha_s(M_Z)$ corresponding to the measured value of $\Lambda_{\overline{\text{MS}}}$ was calculated from the so-called “matching relation” [30] and found to be $\alpha_s(M_Z) = 0.123_{-0.013}^{+0.010}$.

4 Discussion of the results

We have compared our results with the measurements performed by other experiments. The comparison led to the following comments:

- The parameter $\Lambda_{\overline{\text{MS}}}^{(4)} = (411 \pm 200) \text{ MeV}$ of the fit to the xF_3 SF data is in agreement with the NLO analyses with a HT contribution of the CCFR xF_3 data: $\Lambda_{\overline{\text{MS}}}^{(4)} =$

$(381 \pm 53(stat) \pm 17(HT))$ MeV [32] and $\Lambda_{\overline{\text{MS}}}^{(4)} = (428 \pm 158(\text{exp}))$ MeV [26].

- The value of $\Lambda_{\overline{\text{MS}}}^{(4)}$ obtained from the NLO analysis of the xF_3 SF provides the value of the strong interaction constant at the point of a Z boson mass of $\alpha_s(M_Z) = 0.123_{-0.013}^{+0.010}$ which is in agreement with the result of the analysis of the CCFR data $\alpha_s(M_Z) = 0.119 \pm 0.002(\text{exp}) \pm 0.004(\text{theory})$ [32] and with the combined LEP/SLC result $\alpha_s(M_Z) = 0.124 \pm 0.0043$ [33]. Our current measurement is higher by one standard deviation than the value $\alpha_s(M_Z) = 0.113 \pm 0.003(\text{exp}) \pm 0.004(\text{theory})$ [34], obtained in the F_2 structure function analysis of the BCDMS and SLAC data on μN and eN deep-inelastic scattering.

5 Conclusion

We have presented the measurements of the structure functions F_2 and xF_3 in the kinematic range $0.02 < x < 0.65$ and $0.55 < Q^2 < 4.0 \text{ GeV}^2$, obtained from the inclusive deep-inelastic ν_μ and $\bar{\nu}_\mu$ scattering data collected at the IHEP-JINR neutrino detector. The NLO QCD analysis with HT contributions of xF_3 under the assumption of QCD validity in the region of low Q^2 yields $\Lambda_{\overline{\text{MS}}}^{(4)} = (411 \pm 200)$ MeV; the corresponding value of the strong interaction constant is $\alpha_s(M_Z) = 0.123_{-0.013}^{+0.010}$.

Acknowledgements. This work has been supported by the Russian Foundation for Basic Research under grants 96-02-17608, 96-02-18562, 99-01-00091, and by the INTAS under contract 93-1180.

References

1. G. Altarelli, in Proceedings of the ‘‘QCD – 20 Years Later’’ Conference, Aachen, 1992, edited by P.M. Zerwas, H.A. Kastrup (World Scientific, Singapore 1993), v. 1., p. 172
2. S.A. Bunyatov et al., in Proceedings of the International Conference on Neutrino Physics, Balatonfured 1982, v. 2, p. 249
3. D.G. Baratov et al., Sov. J. Technical Phys. **47**, 991 (1977); A.P. Bugorsky et al., Nucl. Instr. and Meth. **146**, 367 (1977)
4. V.B. Anikeev et al., Z. Phys. C **70**, 39 (1996)
5. C.G. Callan, D.J. Gross, Phys. Rev. Lett. **22**, 156 (1969)
6. A. De Rujula et al., Nucl. Phys. B **154**, 394 (1979)
7. H. Abramowicz et al., Z. Phys. C **17**, 283 (1983)
8. A.S. Vovenko et al., Nucl. Instr. and Meth. **212**, 155 (1983)
9. A.J. Buras, K.J.F. Gaemers, Nucl. Phys. B **132**, 249 (1978); K. Varvell et al., Z. Phys. C **36**, 1 (1987)
10. H. Georgi, H.D. Politzer, Phys. Rev. D **14**, 1829 (1976); J. Kaplan, F. Martin, Nucl. Phys. B **115**, 333 (1976); R. Brock, Phys. Rev. Lett. **44**, 1027 (1980)
11. A. Bodek, J.L. Ritchie, Phys. Rev. D **23**, 1070 (1981)
12. J. Blumlein, in Materials of the VIII Workshop on the IHEP-JINR Neutrino Detector, Dubna 1988, p. 115
13. Y.M. Sapunov, Y.M. Sviridov, in Materials of the XVII Workshop on the IHEP-JINR Neutrino Detector, Dubna 1995, p. 81
14. R. Field, R.P. Feynman, Phys. Rev. D **15**, 2590 (1977)
15. M. Gluck, E. Reya, A. Vogt, Z. Phys. C **48**, 471 (1990)
16. G. Parisi, N. Surlas, Nucl. Phys. B **151**, 421 (1979); I.S. Barker, C.B. Langensiepen, G. Shaw, Nucl. Phys. B **186**, 61 (1981); V.G. Krivokhizhin et al., Z. Phys. C **36**, 51 (1987); A. Benvenuti et al. Phys. Lett. B **195** (1987) 97; B **223**, 490 (1989)
17. V.G. Krivokhizhin et al., Z. Phys. C **48**, 347 (1990)
18. A.L. Kataev, A.V. Sidorov, Phys. Lett. B **331**, 179 (1994)
19. O. Nachtmann, Nucl. Phys. B **63**, 237 (1973); H. Georgi, H.D. Politzer, Phys. Rev. D **14**, 1829 (1976); S. Wandzura, Nucl. Phys. B **122**, 412 (1977)
20. F.J. Yndurain, Quantum Chromodynamics (An Introduction to the Theory of Quarks and Gluons) (Springer-Verlag, Berlin 1983), p. 117
21. A. Buras, Rev. Mod. Phys. **52**, 199 (1980)
22. A.L. Kataev et al., Phys. Lett. B **388**, 179 (1996)
23. A.V. Sidorov, JINR Rapid Comm. **80**, 11 (1996)
24. M. Dasgupta, B.R. Webber, Phys. Lett. B **382**, 273 (1996)
25. A.V. Sidorov, Phys. Lett. B **389**, 379 (1996)
26. A.L. Kataev et al., Phys. Lett. B **417**, 374 (1998); INR P0989/98; JINR E2-98-265 (hep-ph/9809500)
27. D.J. Gross, C.H. Llewellyn-Smith, Nucl. Phys. B **14**, 337 (1969). S.G. Gorishny, S.A. Larin, Phys. Lett. B **172**, 109 (1986) E.B. Zijstra, W.L. van Neerven, Phys. Lett. B **297**, 377 (1992)
28. MINUIT, CERN Program Library Long Writeup D 506 (1992)
29. F. James, Interpretation of the Errors on Parameters as Given by MINUIT, Supplement to Long Writeup D 506 (1978)
30. W. Marciano, Phys. Rev. D **29**, 580 (1984)
31. J.H. Kim et al., Phys. Rev. Lett. **81**, 3595 (1998)
32. W.G. Seligman et al., Phys. Rev. Lett. **79**, 1213 (1997)
33. Particle Data Group, C. Caso et al., Eur. Phys. J. C **3**, 85 (1998)
34. M. Virchaux, A. Milsztajn, Phys. Lett. B **274**, 221 (1992)